Published in final edited form as:
Neuroimage 51(3), 1162-1167.
doi: 10.1016/j.neuroimage.2010.03.041

Visually induced gamma-band activity predicts speed of change detection in humans

Nienke Hoogenboom[1,2*], Jan-Mathijs Schoffelen[1,2], Robert Oostenveld[1], and Pascal Fries[1,3]

[1] Donders Institute for Brain, Cognition and Behaviour, Radboud University Nijmegen, 6525 EN Nijmegen, The Netherlands.
[2] Centre for Cognitive Neuroimaging, Department of Psychology, University of Glasgow, G12 8QB Glasgow, United Kingdom.
[3] Ernst-Strüngmann-Institute in Cooperation with the Max-Planck-Society, 60528 Frankfurt, Germany.

*Corresponding author, current address:
Nienke Hoogenboom
Department of Psychology
University of Glasgow
58 Hillhead Street
G12 8QB, Glasgow, UK
E-mail: nienke@psy.gla.ac.uk
Phone: (+44) (0)141 330 2267
Fax: (+44) (0)141 330 4606

Abstract

Groups of activated neurons typically synchronize in the gamma-frequency band (30-100 Hz), and gamma-band synchronization has been implicated in numerous cognitive functions. Those functions are ultimately expressed as behavior and therefore, functional gamma-band synchronization should be directly related to behavior. We recorded the magnetoencephalogram in human subjects and used a visual stimulus to induce occipital gamma-band activity. We found that the strength of this gamma-band activity at a given moment predicted the speed with which the subject was able to report a change in the stimulus. This predictive effect was restricted in time, frequency and space: It started only at 280 ms before the behaviorally relevant stimulus change; It was present only between 50 and 80 Hz; It was significant only in bilateral middle occipital gyrus, while the peak of overall visually induced gamma-band activity was found in the calcarine sulcus. These results suggest that visually induced gamma-band activity is functionally relevant for the efficient transmission of stimulus change information to brain regions issuing the corresponding motor response.

Keywords

MEG, oscillation, rhythm, synchronization, visual cortex.

Introduction

When groups of cortical neurons are activated, they typically engage in neuronal gamma-band synchronization (Gray et al., 1989; Bragin et al., 1995; Fries et al., 2001; Pesaran et al., 2002; Kaiser et al., 2004; Lachaux et al., 2005; Wyart and Tallon-Baudry, 2008). Gamma-band activity is modulated during several cognitive tasks and correspondingly, it has been hypothesized that gamma-band activity subserves the respective cognitive functions mechanistically. Yet, few studies have demonstrated direct consequences of gamma-band synchronization for neuronal processing (Womelsdorf et al., 2007) or behavior (Gonzalez Andino et al., 2005; Schoffelen et al., 2005; Womelsdorf et al., 2006; Hanslmayr et al., 2007). A recent study tested whether the precision of stimulus induced gamma-band synchronization in awake monkey V4 predicted the speed with which a change in the stimulus could be reported behaviorally (Womelsdorf et al., 2006). Trials with a rapid behavioral response showed stronger gamma-band synchronization already before the behaviorally relevant stimulus change. This effect was specific to the gamma-frequency band and not accompanied by changes in neuronal firing rate. It suggests that the gamma-band synchronization, induced locally in V4 through a visual stimulus, is functionally relevant for transmitting stimulus information to downstream brain areas. However, from those results, it is not clear, whether similar effects are present in other brain areas and whether similar effects can be seen in the human brain.

Human rhythmic brain activity, as measured with electroencephalography (EEG), has been studied with regard to its ability to predict behavioral reaction times (RTs). Gonzalez Andino et al. found that reaction times to stimulus onsets could be predicted by gamma-band activity before stimulus onset (Gonzalez Andino et al., 2005). This RT predicting gamma-band activity was localized to a frontoparietal network and therefore might be related to top-down attentional control. Reaction time predictive gamma-band activity was not found in visual cortex, which is in contrast to the findings from monkey microelectrode recordings. This discrepancy might be due to the fact that microelectrode recordings in the monkeys were restricted to visual cortex, but assessed this activity with very high signal-to-noise ratio. Alternatively, the discrepancy might be due to the fact that Gonzalez Andino et al. used pre-stimulus activity to predict RTs to stimulus onset, whereas Womelsdorf et al. used stimulus induced activity to predict RTs to a stimulus change. The presence of a stimulus induces gamma-band activity in visual areas and this might make an RT predictive effect in those areas visible.

We presented subjects with a visual stimulus and recorded visually induced gamma-band activity with MEG (Hoogenboom et al., 2006), while subjects reported stimulus changes. We then investigated whether time-frequency components of this activity predicted behavioral reaction times and estimated the cortical locations of those RT predictive components.

Materials and Methods

Subjects. Twelve healthy volunteers (mean age 23.8, five female) participated in this study. All subjects were right-handed, had normal or corrected-to-normal visual acuity, and none had a history of neurological or psychiatric disorders. The experiment was approved by the local ethics committee, and written informed consent was obtained from every subject.

Experimental paradigm and stimuli. Data for seven of the subjects were taken from an earlier study (Hoogenboom et al., 2006). Data from five additional subjects used essentially the same paradigm, except that stimuli had been further optimized for the induction of gamma-band activity. Each trial started with the presentation of a fixation point (Gaussian of diameter 0.5°). After 500 ms, the fixation point contrast was reduced by 40%, which served as a warning. After another 1500 ms, the fixation point was replaced by a foveal, circular sine wave grating (diameter: 5°; spatial frequency: 2 cycles/° in the first seven subjects and 4 cycles/° in the next five subjects; contrast: 100%). The sine wave grating contracted toward the fixation point (velocity: 1.6 °/s in the first seven subjects and 0.5 °/s in the next five subjects) and this contraction accelerated (velocity step to 2.2 deg/s) at an unpredictable moment between 50 and 3000 ms after stimulus onset. The subjects' task was to press a button with their right index finger within 800 ms of this acceleration. Ten percent of the trials were catch trials in which no acceleration occurred. In order for the trial to be included for further analysis, the subject had to detect the speed change by means of a right hand button-press within 200-800 milliseconds after stimulus acceleration. Subjects were instructed to respond both quickly and accurately. After stimulus offset, subjects received visual feedback on their response for 1000 milliseconds and were encouraged to blink during this period. At the end of each block, visual feedback was given about block number, percentage correct responses, and mean reaction time. A recording session included 6 blocks of 75 trials, and typically lasted for 50 minutes. Stimuli were presented using the 'Presentation' software package (Neurobehavioral Systems, Inc.) in combination with an LCD projector with a vertical refresh rate of 60Hz. Control measurements with a sensitive photodiode showed no 60-Hz component in the luminance time course of the stimuli.

Data acquisition. MEG was recorded using a 151-sensor axial gradiometer system (CTF systems Inc., Port Coquitlam, Canada). The electrooculogram (EOG) was recorded for offline artifact rejection. Data were low-pass filtered at 300 Hz and digitized at 1200 Hz. The subject's head position relative to the sensor array was determined before and after the MEG recording. For source reconstruction, we obtained structural magnetic resonance images from each subject using a 1.5 Tesla whole-body MRI scanner (Siemens, Erlangen, Germany) and co-registered them with the MEG data.

Data analysis: General. All data were analyzed using the FieldTrip open source Matlab toolbox (http://www.ru.nl/fcdonders/fieldtrip) and Matlab 7.1 (MathWorks, Natick, MA). From the continuous MEG data, we defined epochs of interest. Epochs contaminated with artifacts were discarded using semi-automatic routines and power line noise was removed as described previously (Hoogenboom et al., 2006).

Since the subjects' head position with respect to the MEG system varied across subjects, averaging on the sensor level over subjects can cause smearing or cancellation of activity in non-overlapping brain areas. To compensate for these different head positions, the channel-level MEG data were interpolated to a common template gradiometer array, constructed from the average gradiometer position of all twelve datasets, using a minimum-norm projection method. Subsequently, the horizontal and vertical components of the planar gradient were estimated from the axial field distribution, using a nearest neighbor method (Bastiaansen and Knösche, 2000). Rhythmic neuronal activity was estimated by determining the power of the MEG signals. Power spectra were calculated separately for the horizontal and vertical planar gradients and combined to obtain the power at that sensor location regardless of the orientation of the gradient.

Our analysis primarily contrasted visually induced neuronal activity resulting in rapid behavioral responses against activity resulting in slow behavioral responses (behavioral contrast). For comparison, we also provide the contrast between visual stimulation against a baseline without stimulation (stimulation contrast). Both contrasts used analysis approaches and parameters as similar as possible.

Data analysis: Behavioral contrast in time and frequency. We first calculated the behavioral contrast, separately for many time-frequency windows around the behaviorally relevant stimulus speed change. To increase sensitivity, we averaged power over a broad selection of MEG channels overlying visual cortex, namely the 22 occipital channels of the 151-channel CTF system marked with 'O'.

We selected trials that contained a stimulus change and a correct response, i.e. a response between 0.2 and 0.8 s after stimulus change. From those trials, we selected the epochs starting 0.4 s before stimulus change and lasting until the behavioral response (button press). Time-frequency representations (TFRs) of power were calculated using windows of 200 ms moved in steps of 10 milliseconds. For frequencies between 5 and 30 Hz, we tapered with a Hanning window. For frequencies between 30 and 120 Hz, we used multitaper spectral estimation with a spectral concentration of ±12.5 Hz (5 tapers) (Mitra and Pesaran, 1999).

We sorted the trials according to reaction times and contrasted the fastest 25% against the slowest 25%. Per subject, time and frequency point, we performed an independent samples t-test between the log-transformed power values of the two reaction time conditions, across epochs. Across subjects, the t-values were pooled (sum of individual t-values divided by the square root of the number of subjects). Statistical inference was based on a non-parametric randomization test. This test thresholded the time-frequency t-maps at a value of 1.96 (corresponding to a two-sided t-test with an alpha level of 0.05), resulting in time-frequency clusters. The t-values were summed per cluster and used as the test statistic (Nichols and Holmes, 2001; Maris and Oostenveld, 2007). A randomization distribution of this test statistic was determined by randomly exchanging, per subject, the fast and slow reaction time conditions. This was done for all possible permutations given the number of subjects, and for each randomization only the maximal test statistic was retained. An observed cluster was deemed significant if it fell outside the central 95% of this randomization distribution, corresponding to a two-sided random effect test with 5% false positives, corrected for the multiple comparisons across times and frequencies.

Data analysis: Behavioral contrast in space. Based on the time-frequency analysis, we defined a time-frequency window and then tested where in the brain there was a difference in power for that time-frequency window. To this end, we used an adaptive spatial filtering technique in the frequency domain (Gross et al., 2001). A given spatial filter is constructed to pass activity from one source location, while suppressing all other activity. It takes into account the forward model at the location of interest (the leadfield matrix) and the cross-spectral density (CSD) between all MEG signal pairs at the frequency of interest. The CSD matrix was determined for the time-frequency window from 0.3 s before the stimulus change to 0.2 s after the change and from 50 to 80 Hz. Multitaper techniques provided spectral concentration of ±15 Hz (15 tapers). The leadfield matrix was determined for a realistically shaped single-shell volume conduction model (Nolte, 2003), derived from the individual subject's structural MRI.

Spatial filters were constructed to estimate source activity for a grid of locations. This grid was constructed as a regular 5-mm grid in the Montreal Neurological Institute (MNI) template brain. Each subject's structural MRI was linearly warped onto this template, the inverse of this warp was applied to the template grid and the spatial filters were constructed for the inversely warped grid locations in the individual head coordinates using the individual subject's volume conduction model. Source parameters estimated in this way per subject were combined across subjects per grid position and displayed on the MNI template brain.

The filters were determined based on the CSD matrix averaged over all trials of a given subject. CSD matrices of single trials were then projected through those filters, providing single trial estimates of source power. Statistical testing proceeded identical to the time-frequency case, except that the two dimentions time and frequency were replaced by the three spatial dimensions.

Data analysis: Stimulation contrast. For comparison, the same analyses were repeated for the stimulation contrast, contrasting visual stimulation with the baseline. The only differences were: 1.) The time-frequency analysis extended from 0.1 s before stimulus onset until 1.1 s seconds past onset and compared this to a baseline window from 1.1 s before stimulus onset until 0.1 s after onset. 2.) The within-subject t-tests were dependent-samples t-tests (rather than independent-samples t-tests), because each stimulation period had a corresponding baseline period. 3.) The source analysis contrasted two time-frequency windows: A stimulation window from 0.5 to 1 s after stimulus onset with a baseline window from 0.5 to 0 s before onset.

Data analysis: Trial-by-trial correlation. In addition to the contrast between the fastest and slowest trials, we were also interested in the trial-by-trial correlation between gamma-band power and reaction time. We estimated gamma-band power at the source level for each trial separately as described above. We then averaged gamma-band power over the two clusters of voxels that had shown significantly different gamma-band power between fast and slow response trials on the group level. This source estimate of gamma-band power was obtained for each trial of each subject separately. Subsequently, we calculated the Pearson correlation coefficient between source gamma-band power (log transformed) and RT across trials, separately per subject. Finally, we tested the distribution of correlation coefficients across subjects against the null hypothesis of zero mean, using a two-sided t-test.

Results

The effect of visual stimulation on rhythmic activity in human occipital cortex

Visually induced human gamma-band activity has been described previously (Kaiser et al., 2004; Lachaux et al., 2005; Wyart and Tallon-Baudry, 2008) and has been localized in time, frequency and space (Hoogenboom et al., 2006). We characterize the visually induced gamma-band activity here for this group of subjects and the methods used, to allow direct comparison with the analysis of reaction time (RT) related gamma-band effects, described below.

Time-frequency analysis. Visual stimulation induced a decrease in 10-30 Hz alpha- and beta-band activity and an increase in 40-120 Hz gamma-band activity in occipital MEG sensors (Fig. 1*A*). The gamma-band response was clearly band-limited, with a spectral width of the main response of about 30 Hz in the group average and typically less than that in individual subjects [data not shown, but see (Hoogenboom et al., 2006)]. The gamma-band increase slightly preceded the alpha/beta-band decrease, but both were sustained for the duration of stimulation. The gamma-band response exhibited a characteristic drop in frequency with time after stimulus onset (Pesaran et al., 2002; Hoogenboom et al., 2006), and settled to a sustained peak frequency around 65 Hz.

Source analysis. The visually induced gamma-band activity originated primarily from primary and secondary visual cortex (Brodmann areas 17 and 18) (Fig. 1*B*).

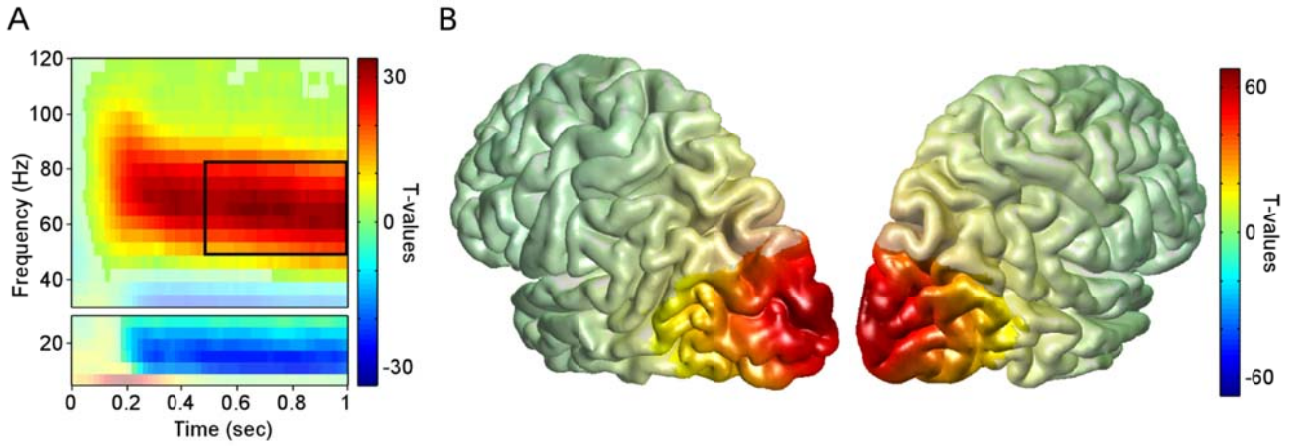

Figure 1 The effect of visual processing. (A) Time-frequency representations of the pooled t-values from the comparison to pre-stimulus baseline. (B) Source estimate for the time-frequency window as marked in A. Gray shading reveals significant effects.

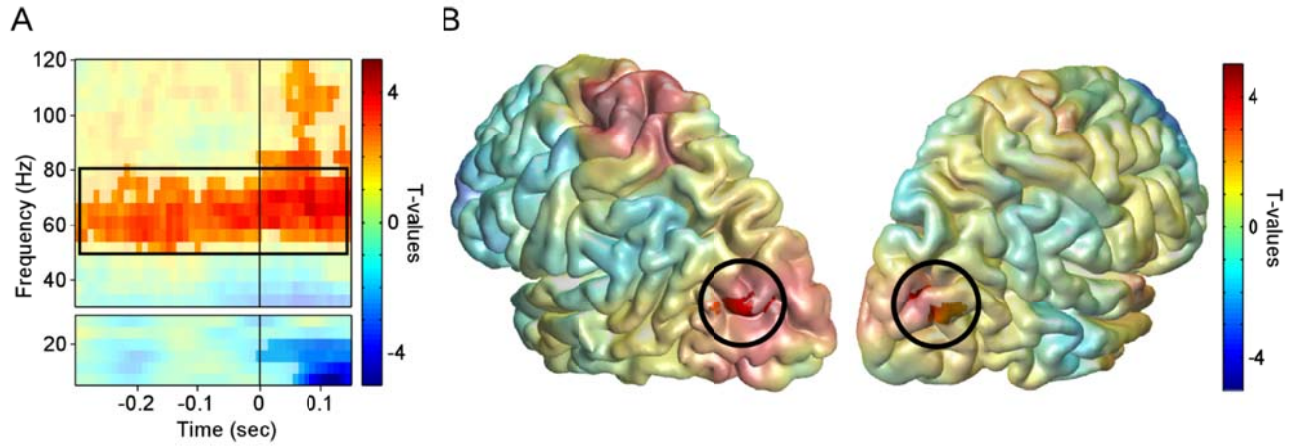

Figure 2 The predictive effect for behavioral response times. Same format as Fig. 1, but showing the comparison between trials with fast versus slow behavioral responses.

The relation between visually induced gamma-band activity and behavioral response times

To assess the relation between rhythmic brain activity and reaction times, trials were sorted according to their reaction times and separated into quartiles. The 25% fastest trials (RT mean: 315 ms, sd: 41.5 ms) and the 25% slowest trials (RT mean 525 ms, sd 92.7 ms) were contrasted.

Time-frequency analysis. To investigate the time-frequency pattern of RT-predictive rhythmic activity, we aligned this analysis to the stimulus change that provided the go-cue, and limited it to data obtained before the behavioral response. Faster behavioral responses were preceded by enhanced gamma-band activity (Fig. 2*A*). The increased gamma-band activity was present already more than 250 ms before the stimulus change, i.e. at a time when the ±100 ms analysis window did not yet encompass the stimulus change itself. The RT-predictive gamma-band activity occurred in a stable frequency range around 65 Hz. Only between 50 and 100 ms after the stimulus change, additional, higher frequency activity was also RT-predictive. At and shortly after the stimulus change, alpha- and low beta-band activity was reduced in trials

with fast responses. The respective analysis windows encompassed the stimulus change and the neuronal response to it.

Source analysis. The enhanced gamma-band activity preceding faster behavioral responses originated from the middle occipital gyrus of both hemispheres (Fig. 2*B*). While these two regions were the only ones reaching statistical significance after multiple comparison correction, the pattern of (non-significant) RT-predictive source gamma power shows an interesting spatial pattern: A tendency for enhanced gamma-band activity occurred in the left motor cortex, contralateral to the response hand, along bilateral intraparietal sulcus, and in bilateral occipito-temporal cortex. By contrast, a tendency for reduced gamma-band activity occurred bilaterally around the temporo-parietal junction and in left lateral prefrontal cortex. It should be noted though, that these tendencies were not sufficiently consistent across subjects to warrant firm conclusions.

Trial-by-trial analysis. In order to test whether trial-by-trial variability in gamma band power predicted part of the trial-by-trial variability in behavioral response times, we performed a direct correlation analysis (using log-transformed source power estimates, see Methods for details). Behavioral reaction times correlated with the strength of gamma-band power (mean $r=-0.07$, $p<0.05$, two-tailed one-sample t-test in this and the subsequent tests). However, part of this correlation might be only apparent and might in fact be due to a common dependence of both gamma-band power and RT on the latency (post stimulus onset) of the behaviorally relevant stimulus change. With increasing latency, reaction times might decrease and gamma-band power increase. The latency of stimulus change was correlated with RT (mean $r=-0.16$, $p<0.01$), but showed only a tendency to correlate with gamma-band power (mean $r=0.07$, $p=0.0502$). To eliminate the common linear dependence of RT and gamma-band power on latency, we determined the partial correlation coefficient between gamma-band power and RT, after partializing for the latency of stimulus change. We found that gamma-band power correlated with RT also after this partialization, suggesting that their correlation is not solely due to a common relation to the latency (mean $r=-0.06$, $p<0.05$).

Discussion

We used a visual stimulus to produce spectral perturbations of human visual cortical activity. We assessed brain activity with MEG and tested which spectral components predicted the speed with which an unpredictable stimulus change was reported behaviorally. We found that specifically the strength of gamma-band (50-80 Hz) activity predicted short behavioral response times. We estimated the neuronal sources of the RT predicting gamma-band component and found them in bilateral middle occipital gyrus. By contrast, the comparison between stimulation and baseline revealed a spatial peak of gamma-band activity in the calcarine sulcus.

One potential concern is that the observed effect is due to nonspecific slow fluctuations between arousal and drowsiness. Enhanced arousal might well lead to shortened RTs and to enhanced gamma-band activity, thereby explaining the observed negative relation between them. However, there are several reasons why this explanation is unlikely. In our time-frequency analysis, the RT-predictive effect in the gamma-band increased in strength and significance within few hundred milliseconds before the stimulus change to peak around 80 ms after the stimulus change event, at a time when information about the stimulus change is arriving in early visual cortices. This temporal pattern rules out at least slow fluctuations in arousal as the underlying cause. Also the spatial analysis revealed a high specificity that appears inconsistent with being an effect of general arousal: It revealed significant sources that were bilateral, but restricted to the middle occipital gyrus.

The temporal, spectral and spatial specificity of the observed effect is consistent with a previous report of RT-predictive gamma-band activity in area V4 of awake monkeys (Womelsdorf et al., 2006). In

V4, neurons are activated only by stimuli in a restricted region of the contralateral visual field. Therefore, this study performed a control analysis in which one stimulus activated the recorded neurons, but a second stimulus was behaviorally relevant, i.e. triggered behavioral responses. When behavioral responses to this second stimulus were particularly fast, gamma-band activity induced by the other stimulus was particularly weak. This provided direct evidence that the observed effect was spatially highly specific and not due to fluctuations between arousal and drowsiness.

Our results differ from those of an earlier study using pre-stimulus EEG to predict RTs to stimulus onsets (Gonzalez Andino et al., 2005). While also this earlier study found short RTs to be predicted by enhanced gamma-band activity, the estimated sources were restricted to a fronto-parietal network and thereby most likely reflecting the activity of an attentional top-down control. The difference in results is most likely due to a difference in design. While Gonzalez Andino predicted RTs to stimulus onsets by pre-stimulus gamma, we predicted RTs to stimulus changes by gamma-band activity induced by an ongoing stimulus. Our approach enabled us to reveal RT predictive gamma-band activity in human visual cortex and its spatial focus in middle occipital gyrus.

Regarding the mechanisms behind the RT predictive modulations in gamma-band activity, we differentiate between several aspects: The mechanisms that produce gamma-band activity, those that produce spontaneous modulations in its strength and those that link it to behavioral efficiency. The mechanisms behind gamma-band synchronization itself have been well studied (Whittington et al., 1995; Tiesinga et al., 2001; Csicsvari et al., 2003; Hasenstaub et al., 2005; Bartos et al., 2007). In short, activated interneuron networks can produce gamma-band activity and impose it on local networks. Their synchronization properties can be supported by gap junctions. Modulations of the strength of this gamma-band synchronization can be induced by modulations in the level of network excitation, or in the level of several neuromodulators, in particular acetylcholine (Rodriguez et al., 2004). Which of those modulatory mechanisms is behind the RT predictive gamma-band modulation in our data is not clear. The link between the enhanced gamma-band activity and shortened RTs is most likely due to the fact that gamma-band synchronization supports neuronal communication (Engel et al., 2001; Salinas and Sejnowski, 2001; Fries, 2005; Womelsdorf et al., 2007; Börgers and Kopell, 2008). Gamma-band synchronization of a local neuronal group renders inputs to target neurons synchronous and thereby particularly effective. Furthermore, gamma-band synchronization of local inhibitory interneurons leaves periods of disinhibition in which neurons are able to interact. Finally, strong local gamma-band synchronization might entrain distant target neuron groups into the same rhythm and thereby assure optimal communication by temporally aligning their periods of disinhibition.

In conclusion, we have found that the strength of gamma-band activity in early to intermediate visual cortex predicted a small but significant fraction of the variability in the efficiency with which visual information was translated into a behavioral action. We characterized this RT predictive gamma-band activity in time, frequency and space and found it highly specific along each of those dimensions. These results lend further support to the notion that gamma-band activity plays a functional role for neuronal communication.

Funding

This work was supported by the Netherlands Organization for Scientific Research [452-03-344, 051-02-050 to P.F.]; the European Science Foundation [044-035-003 to P.F.]; the Danish Technical Research Council [26-01-0092 to R.O.]; the Ernst-Strüngmann-Institute Ltd.

Acknowledgements

We thank O. Jensen and J.R. Vidal for helpful discussions and suggestions.

Reference List

Bartos, M., Vida, I., Jonas, P., 2007. Synaptic mechanisms of synchronized gamma oscillations in inhibitory interneuron networks. Nat Rev Neurosci 8, 45-56.

Bastiaansen, M.C., Knösche, T.R., 2000. Tangential derivative mapping of axial MEG applied to event-related desynchronization research. Clin Neurophysiol 111, 1300-1305.

Börgers, C., Kopell, N.J., 2008. Gamma oscillations and stimulus selection. Neural Comput 20, 383-414.

Bragin, A., Jando, G., Nadasdy, Z., Hetke, J., Wise, K., Buzsáki, G., 1995. Gamma (40-100 Hz) oscillation in the hippocampus of the behaving rat. J Neurosci 15, 47-60.

Csicsvari, J., Jamieson, B., Wise, K.D., Buzsáki, G., 2003. Mechanisms of gamma oscillations in the hippocampus of the behaving rat. Neuron 37, 311-322.

Engel, A.K., Fries, P., Singer, W., 2001. Dynamic predictions, oscillations and synchrony in top-down processing. Nat Rev Neurosci 2, 704-716.

Fries, P., 2005. A mechanism for cognitive dynamics: neuronal communication through neuronal coherence. Trends Cogn Sci 9, 474-480.

Fries, P., Reynolds, J.H., Rorie, A.E., Desimone, R., 2001. Modulation of oscillatory neuronal synchronization by selective visual attention. Science 291, 1560-1563.

Gonzalez Andino, S.L., Michel, C.M., Thut, G., Landis, T., Grave, dP., 2005. Prediction of response speed by anticipatory high-frequency (gamma band) oscillations in the human brain. Hum Brain Mapp 24, 50-58.

Gray, C.M., König, P., Engel, A.K., Singer, W., 1989. Oscillatory responses in cat visual cortex exhibit inter-columnar synchronization which reflects global stimulus properties. Nature 338, 334-337.

Gross, J., Kujala, J., Hamalainen, M., Timmermann, L., Schnitzler, A., Salmelin, R., 2001. Dynamic imaging of coherent sources: Studying neural interactions in the human brain. Proc Natl Acad Sci USA 98, 694-699.

Hanslmayr, S., Aslan, A., Staudigl, T., Klimesch, W., Herrmann, C.S., Bäuml, K.H., 2007. Prestimulus oscillations predict visual perception performance between and within subjects. NeuroImage 37, 1465-1473.

Hasenstaub, A., Shu, Y., Haider, B., Kraushaar, U., Duque, A., McCormick, D.A., 2005. Inhibitory postsynaptic potentials carry synchronized frequency information in active cortical networks. Neuron 47, 423-435.

Hoogenboom, N., Schoffelen, J.M., Oostenveld, R., Parkes, L.M., Fries, P., 2006. Localizing human visual gamma-band activity in frequency, time and space. NeuroImage 29, 764-773.

Kaiser, J., Bühler, M., Lutzenberger, W., 2004. Magnetoencephalographic gamma-band responses to illusory triangles in humans. NeuroImage 23, 551-560.

Lachaux, J.P., George, N., Tallon-Baudry, C., Martinerie, J., Hugueville, L., Minotti, L., Kahane, P., Renault, B., 2005. The many faces of the gamma band response to complex visual stimuli. NeuroImage 25, 491-501.

Maris, E., Oostenveld, R., 2007. Nonparametric statistical testing of EEG- and MEG-data. J Neurosci Methods 164, 177-190.

Mitra, P.P., Pesaran, B., 1999. Analysis of dynamic brain imaging data. Biophys J 76, 691-708.

Nichols, T.E., Holmes, A.P., 2001. Nonparametric permutation tests for functional neuroimaging: a primer with examples. Hum Brain Mapp 15, 1-25.

Nolte, G., 2003. The magnetic lead field theorem in the quasi-static approximation and its use for magnetoencephalography forward calculation in realistic volume conductors. Phys Med Biol 48, 3637-3652.

Pesaran, B., Pezaris, J.S., Sahani, M., Mitra, P.P., Andersen, R.A., 2002. Temporal structure in neuronal activity during working memory in macaque parietal cortex. Nat Neurosci 5, 805-811.

Rodriguez, R., Kallenbach, U., Singer, W., Munk, M.H., 2004. Short- and long-term effects of cholinergic modulation on gamma oscillations and response synchronization in the visual cortex. J Neurosci 24, 10369-10378.

Salinas, E., Sejnowski, T.J., 2001. Correlated neuronal activity and the flow of neural information. Nat Rev Neurosci 2, 539-550.

Schoffelen, J.M., Oostenveld, R., Fries, P., 2005. Neuronal coherence as a mechanism of effective corticospinal interaction. Science 308, 111-113.

Tiesinga, P.H., Fellous, J.M., José, J.V., Sejnowski, T.J., 2001. Computational model of carbachol-induced delta, theta, and gamma oscillations in the hippocampus. Hippocampus 11, 251-274.

Whittington, M.A., Traub, R.D., Jefferys, J.G., 1995. Synchronized oscillations in interneuron networks driven by metabotropic glutamate receptor activation. Nature 373, 612-615.

Womelsdorf, T., Fries, P., Mitra, P.P., Desimone, R., 2006. Gamma-band synchronization in visual cortex predicts speed of change detection. Nature 439, 733-736.

Womelsdorf, T., Schoffelen, J.M., Oostenveld, R., Singer, W., Desimone, R., Engel, A.K., Fries, P., 2007. Modulation of neuronal interactions through neuronal synchronization. Science 316, 1609-1612.

Wyart, V., Tallon-Baudry, C., 2008. Neural dissociation between visual awareness and spatial attention. J Neurosci 28, 2667-2679.